Journal of Controlled Release 366 (2024) 611–620

Contents lists available at ScienceDirect

Journal of Controlled Release

journal homepage: www.elsevier.com/locate/jconrel

Polyethylene glycol (PEG) as a broad applicability marker for LC–MS/MS-based biodistribution analysis of nanomedicines

Astrid Hyldbakk [a,b], Terkel Hansen [a], Sjoerd Hak [a,c], Sven Even F. Borgos [a,*]

[a] Department of Biotechnology and Nanomedicine, SINTEF Industry, Trondheim, Norway
[b] Department of Physics, Norwegian University of Science and Technology (NTNU), Trondheim, Norway
[c] Department of Circulation and Medical Imaging, Norwegian University of Science and Technology (NTNU), Trondheim, Norway

ARTICLE INFO

Keywords:
Nanomedicine
Drug release
Stability
Biodistribution
PEG
PEGylation
Polyethylene glycol
Mass spectrometry

ABSTRACT

Polyethylene glycol (PEG) conjugation (PEGylation) is a well-established strategy to improve the pharmacokinetic and biocompatibility properties of a wide variety of nanomedicines and therapeutic peptides and proteins. This broad use makes PEG an attractive 'allround' candidate marker for the biodistribution of such PEGylated compounds. This paper presents the development of a novel strategy for PEG quantification in biological matrices. The methodology is based on sample hydrolysis which both decomposes the sample matrix and degrades PEGylated analytes to specific molecular fragments more suitable for detection by LC–MS/MS. Method versatility was demonstrated by applying it to a wide variety of PEGylated compounds, including polymeric poly (ethylbutyl cyanoacrylate) (PEBCA) nanoparticles, lipidic nanoparticles (Doxil®, LipImage 815™ and lipid nanoparticles for nucleic acid delivery) and the antibody Cimzia®. Method applicability was assessed by analyzing plasma and tissue samples from a comprehensive drug biodistribution study in rats, of both PEBCA and LipImage 815™ nanoparticles. The results demonstrated the method's utility for biodistribution studies on PEG. Importantly, by using the method described herein in tandem with quantification of nanoparticle payloads, we showed that this approach can provide detailed understanding of various critical aspects of the in vivo behavior of PEGylated nanomedicines, such as drug release and particle stability. Together, the presented results demonstrate the novel method as a robust, versatile and generic approach for biodistribution analysis of PEGylated therapeutics.

1. Introduction

Nanomedicines, i.e. biocompatible nanoparticles applied for in vivo delivery of medicine, have been used in the clinic for >25 years. The clinical approval of the liposomal doxorubicin formulation Doxil® in 1995 demonstrated the potential of nanomedicines, by significantly improving the safety and efficacy of conventional doxorubicin (1). Yet, it was the unprecedented success of the mRNA-based COVID-19 vaccines that unambiguously demonstrated the utility of nanomedicine. As of now, >12 billion vaccine doses have been administered globally (2), with outstanding safety and efficacy profiles. A recent study estimated that during the first year of vaccinations alone, 19.8 million deaths were avoided due to the vaccines (3); the mRNA-based vaccines are generally considered to have superior efficacy.

Encapsulating an active pharmaceutical ingredient (API) in nanoparticles has several potential advantages. The protection of the API from premature degradation in the body is crucial in the case of e.g. mRNA-based therapies. The prevention of off-target toxicity can be another key advantage, as in the case of Doxil®, showing reduced cardiotoxicity as compared to administration of free doxorubicin (1). Encapsulation of the API can dramatically change its absorption, distribution, metabolism and excretion (ADME) and improve therapeutic effect, but will generally complicate prediction and modelling of its pharmacokinetic properties and biodistribution. For small molecule APIs, robust modelling frameworks exist; the same is not yet the case for nanomedicines, although efforts are under way to build these (4,5). One crucial aspect to understand is the in vivo release of API from the nanoparticle, e.g. by diffusion or particle disintegration. Although advanced methods exist to measure the release of API in vitro and in vivo into plasma (6,7), these are generally not applicable to biodistribution into tissue. Analysis of nanomedicine ADME has mostly relied on quantification of the API, and not on the nanocarrier. This approach

* Corresponding author.
E-mail address: sveneven.borgos@sintef.no (S.E.F. Borgos).

https://doi.org/10.1016/j.jconrel.2024.01.016
Received 3 August 2023; Received in revised form 15 December 2023; Accepted 9 January 2024
Available online 13 January 2024

does, however, not give information on whether the API is encapsulated or released from its nanocarrier. Only the latter is able to exert its pharmaceutical activity, and a distinction should therefore be made between the two variants. Additionally, drug release will generally alter the ADME of the API dramatically, both in terms of biodistribution and pharmacokinetics.

PEG is a synthetic polymer, ubiquitously used in chemical and pharmaceutical industry. Its high water solubility, non-toxicity, non-immunogenicity and flexibility in polymer length and chemical modification have given PEG an indispensable role as solubilizer and stabilizer in a wide range of applications, including consumer products and pharmaceuticals (8,9). PEG has been approved for intravenous, oral and dermal administration in humans in most countries (10). Conjugation of PEG (i.e. PEGylation) to therapeutic agents such as small molecules, proteins, peptides and nanoparticles has been shown to significantly improve their pharmacokinetic and pharmacological profiles. As of today, about 30 PEGylated pharmaceutics have reached the market (10–12); this includes some of the most-selling antibody and protein therapeutics (13). PEGylation offers a hydrophilic hydrated steric surface barrier that shields the therapeutic agent from biological inactivation by proteolysis, metabolism, and mononuclear phagocyte system (MPS) uptake, commonly referred to as the 'stealth effect' (8). Additionally, PEGylation can increase the aqueous solubility of the therapeutic agent and reduce immunogenicity (10,11,14), although recent work has raised some concerns about potential adverse immune reactions against the PEG moities per se, such as anti-PEG antibodies (15) and hypersensitivity more broadly (16). For small polymeric PEGylated nanoparticles, PEG molecular weight has been shown to have a clear impact on tumor accumulation, biodistribution and pharmacokinetics, via the so-called EPR effect. Which, due to increased vascular permeability and poor lymphatic drainage in tumor tissue, can improve drug accumulation in these tissues compared to that in healthy tissue (17).

Current PEGylated nanomedicines in clinical use and testing encompass a wide range of particle materials and substructures, like liposomes (e.g. Doxil®, Onivyde®, Lipoplatin®), lipid nanoparticles (LNPs) based on ionizable lipids (e.g. Onpattro®, the BioNTech-Pfizer COVID-19 vaccine Comirnaty® and the Moderna COVID-19 vaccine Spikevax® (18)), dendrimers (19), polymeric micelles (20) and other polymeric nanoparticles (21). These examples cover a large chemical space, and the only common compositional motif is the presence of polyethylene glycol (PEG). PEG is also present on the majority of nanomedicines in preclinical development. It should be noted that both for nanomedicines and other advanced therapeutics, PEG is in most cases covalently attached to other molecules, which can range from lipids to large synthetic polymers or proteins, thus constituting a very heterogeneous spectrum of compounds. This makes a unified detection and quantification of these PEG-containing molecules exceedingly difficult.

The lack of specific chromophores makes PEG very hard to discern from endogenous molecules by optical techniques, which are generally preferred for sensitivity. Also, the PEG molecule has low chemical and biochemical reactivity and detection by specific chemical or enzymatic derivatization is hardly possible, although anti-PEG enzyme-linked immunosorbent assays (ELISAs) are available. Furthermore, upon sufficiently harsh chemical treatments, scission of the PEG chains will occur (22). There is a need for methodologies that enable specific quantification of PEG in biological matrices. As some tissues might have low accumulation of PEG, both high-recovery sample preparation and sensitive and specific detection methods are required. Biological tissues vary across a wide range of biochemical and mechanical properties. Therefore, a robust, versatile and generic extraction method for biodistribution studies is highly desirable. Here, we describe the development of a novel, near-universal strategy for biodistribution analyses of nanomedicines and other PEGylated therapeutics, based on liquid chromatography coupled to tandem mass spectrometry (LC–MS/MS). A comprehensive sample hydrolysis step is included with the dual objective of releasing characteristic, PEG-specific molecular fragments from a representative variety of PEGylated analytes, and simultaneously extract the analytes from virtually all tissue types with low background interference, e.g. from matrix proteins. A somewhat related approach was used by Berrecoso et al (23) to comprehensively analyze composition of nanocapsules, some of which contained PEGylated compounds, although only in pristine dispersion and with no quantification of the PEG moieties.

We showed our method can be used to quantify PEG in several commercially available and different classes of PEGylated therapeutics, including the liposome formulation Doxil®, the antibody Cimzia® and lipid nanoparticles (LNPs) used for nucleic acid delivery. To demonstrate the convenience of the method in biodistribution studies, it was successfully applied on biological plasma and tissue samples from a comprehensive drug biodistribution study in rats, including both polymeric (poly(ethylbutyl cyanoacrylate; PEBCA) and lipidic (LipImage 815™, henceforth LipImage) nanoparticles (24). Finally, we demonstrated the method's utility beyond biodistribution studies by applying it in tandem with quantification of nanoparticle payloads. PEBCA nanoparticles containing the antineoplastic drug cabazitaxel (PEBCA-CBZ) constitute a well-studied and promising polymer-based drug delivery system (25,26), whereas LipImage is a solid-lipid-based nanoformulation of the near-infrared dye IR780-oleyl, for use in fluorescence-guided surgery (27). The results demonstrated our method can be used for developing novel understanding of nanoparticle in vivo stability and drug release.

2. Methods

2.1. Processing of PEGylated example compounds

Initial method development was performed on pure PEG chains of different length, including PEG600 (81,180, Sigma-Aldrich, Darmstadt, Germany), PEG1000 (8.07488, VWR, Radnor, Pennsylvania, US) and PEG3000 (81,227, Sigma-Aldrich). The two PEGylated nanoformulations LipImage (synthesized as described by Jacquart et al. (27)) and PEBCA nanoparticles (synthesized as described by Snipstad et al. (25) were chosen for further method development. This also included their PEG constituents Myrj S40 (Croda Uniqema) (LipImage), Brij L23 (Sigma-Aldrich) (PEBCA nanoparticles) and Kolliphor HS15 (Sigma-Aldrich) (PEBCA nanoparticles). The chemical structures of the PEG compounds are shown in Fig. S1. Several PEGylated formulations were used for method development and to study method versatility and applicability. These included Doxil®/Caelyx® (doxorubicin; Janssen-Cilag International NV, Belgium), Cimzia® (certolizumab; UCB, Brussels, Belgium) and LNPs, produced as previously described (28).

Pure compounds and nanoparticles were diluted to a concentration of 1 mg/mL in distilled water or homogenized liver tissue from rats (as described in the "Biodistribution study in rats" section below) before further use. Hydrolysis was performed by mixing the sample with 9 M H_2SO_4 (1:2 volume ratio) in glass culture tubes (Wheaton) to reach a final acid concentration of 6 M. All tubes were capped with rubber septum stoppers covered by open top screw caps (Bellco Glass) before 24-h or 48-h incubation at 105 °C. Sample sediments were removed by filtration (regenerated cellulose filters, 0.45 μm pore size, VWR) before sample pH was buffered at approx. 6 by addition of 10 M ammonium acetate and 5 M NaOH (1:1:1 volume ratios) in HPLC vials.

2.2. High resolution qualitative mass spectrometry analysis

Qualitative high resolution mass spectrometry analysis was acquired utilizing a Bruker Impact II mass spectrometer (Bruker Daltonik GmbH, Bremen, Germany) coupled to an Agilent HPLC (Agilent Technologies, Inc., Santa Clara, US) as a starting point for development of a MS quantification method. PEG chain separation was achieved on a reverse-phase Ascentis Express phenyl-hexyl column (4.6 mm × 15 cm, 2.7 μm

pore size, Sigma-Aldrich) kept at 55°, a constant flow rate of 0.7 mL/min and with 2 μL sample injection. Mobile phase A consisted of ammonium acetate (50 mM in distilled water) and mobile phase B was methanol and acetonitrile (90:10 volume ratio). The mobile phase gradient started with 40% B for 1 min, a linear increase to 60% B over 4 min and a linear increase to 75% B over 5 min. After that, the amount of mobile phase B was increased to 100% and maintained at 100% for 2 min prior to column re-equilibration. This resulted in a total runtime of 14.25 min per sample.

All MS spectra were acquired from *m/z* 20 to m/z 1300 at 12 Hz. Data dependent MS2 spectra were acquired for signals over 400 counts pr 1000 sum spectra and excluded after 3 spectra for 0.2 min. Cycle time was set for 0.5 s and MS2 repetitions was set to 1×. Precursor isolation window was set to 2.5 *m/z* and collision energy was set to 20 eV for m/z values below 1000, and 30 eV for m/z values over 1000. Maximum MS2 acquisition was set to 20 Hz for target intensities over 20,000 and 12 Hz for target intensities below threshold. The MS was operated in positive electrospray ionization (ESI) mode, with the following settings: gas temperature at 220 °C, gas flow at 10 L/min, nebulizer at 2.2 Bar, capillary current of 4500 V and end plate offset of 500 V.

2.3. Quantitative mass spectrometry analysis

Quantitative MS was performed on an Agilent 1290 HPLC system coupled to an Agilent 6490 triple quadrupole MS. Chromatographic separation was achieved using the same settings as for the QTOF analyses described above. The MS was operated in positive electrospray ionization (ESI) mode (Agilent Jetstream) with the following settings: gas temperature at 200 °C, gas flow at 11 L/min, nebulizer at 20 psi, sheath gas temperature at 400 °C, sheath gas flow at 12 L/min, capillary current of 4500 nA, nozzle voltage of 0 V, high pressure RF of 150 V and low pressure RF of 60 V. To allow quantitative analysis of PEG, a series of PEG-specific multiple reaction monitoring (MRM) transitions were selected (Table 1), based on the results from the qualitative LC–MS/MS mass analyses. Optimization of collision energy values for each transition was performed by the Agilent MassHunter Optimizer software. Dynamic MRM, with retention time windows for each analyte, was applied to reduce the number of concurrent ion transitions and hence potentially improve analyte sensitivity.

2.4. Biodistribution study in rats

Tissue samples were collected from a previous in vivo study comparing the biodistribution of IR780-oleyl and CBZ in healthy rats (24). In this study, the nanoparticle payload in different tissues was determined by LC–MS/MS analysis of IR780-oleyl and CBZ in tissue homogenates after administration of IR780-oleyl as the LipImage formulation (192 mg lipid/kg and 0.46 mg IR780-oleyl/kg), or CBZ as PEBCA-CBZ (30.5 mg NPs/kg and 3.5 mg CBZ/kg). The content of payload and PEG in the nanopreparations were 43.2 mg Myrj S40/mL and 0.23 mg IR-780-oleyl/mL (LipImage) and 6.1 mg Kolliphor HS15/mL, 6.1 mg Brij L23/mL and 12.3 mg CBZ/mg (PEBCA-CBZ). In the current study, a selection of samples, including blood plasma, heart, kidney, spleen, lung and liver tissues from animals euthanized at 1 h, 1 day, 2 days, 4 days and 14 days after injection ($n = 4$ per timepoint) was chosen for PEG biodistribution studies. Blank rat plasma, blank rat tissue homogenates and distilled water (control sample) were spiked with LipImage or PEBCA-CBZ to give standard curves with final concentrations ranging between 10 and 100,000 ng nanoformulation/mL. All samples and standards were hydrolyzed by the same protocol as described above, with plasma and homogenized tissue samples being mixed with 9 M H_2SO_4 at 1:2 volume ratios in glass culture tubes.

Quantification was performed against these hydrolyzed nanoformulation standard curves, rather than the single PEGylated compounds, thus directly yielding data as concentration of nanoformulation equivalents.

Table 1
PEG-specific MRM (multiple reaction monitoring) transitions used for PEG detection and quantification.

PEG chain	Nominal mass	Precursor ion (*m/z*) (Ammonium adduct)	Product ion (m/z)	Retention time (min)	Collision energy (V)
PEG9	414	432	89	3.86	20
PEG10	458	476	89	4.29	24
PEG11	502	520	89	4.72	24
PEG12	546	564	89	5.18	24
PEG13	590	608	89	5.55	24
PEG14	634	652	89	5.94	24
PEG15	678	696	89	6.31	24
PEG16	722	740	89	6.67	36
PEG17	766	784	89	6.99	40
PEG18	810	828	89	7.25	40
PEG19	854	872	89	7.52	44
PEG20	898	916	89	7.85	44
PEG21	942	960	89	8.16	48
PEG22	986	1004	89	8.43	52
PEG23	1030	1048	89	8.72	64
PEG24	1074	1092	89	9.00	64
PEG25	1118	1136	89	9.27	64

3. Results and discussion

3.1. Hydrolysis allows for specific PEG chain cleavage and tissue degradation

Initial qualitative characterization of PEG compounds was performed on neat PEG compounds of varying chain lengths (PEG600, PEG1000 and PEG3000) and example PEG conjugates with clinical relevance (Myrj S40, Brij L23 and Kolliphor HS15) (Fig. S1). All native PEG compounds gave complex spectra in the mass range between *m/z* 450 and m/z 1000 (Fig. S2) illustrating the heterogeneous nature of PEG and multiple charges of each molecule. These spectra were therefore not suited for qualitative or quantitative analysis, in line with previous observations (29–31).

To improve the detection limits and homogenize the analytical pipeline for PEGylated therapeutics, a hydrolysis protocol was developed to release the PEG moiety from its conjugates. PEG is frequently conjugated through either ester or amide groups, and it was hypothesized that these bonds could be cleaved by acidic hydrolysis. Initial tests showed that hydrochloric acid (HCl) hydrolysis could decrease the complexity of the original PEG spectra, resulting in the characteristic pattern of compounds with an iterative increase of *m/z* 44 Da for singly charged ions eluted at progressively longer retention times. This corresponded to the repeating -C_2H_4O- ethylene glycol unit of PEG. Acidic hydrolysis was initially performed with HCl, as it is frequently used in established protocols for protein hydrolysis. It was, however, observed that HCl led to the formation of chlorinated PEG compounds (.

Fig. 1). This chlorination was incomplete and poorly reproducible under the conditions tested, and thus not desirable from an analytical point of view. Hydrolysis with sulfuric acid (H_2SO_4) was tested as an alternative, yielding only linear PEG moieties, and as no sulphate containing compounds or other impurities from the hydrolysis step could be observed, sulfuric acid was chosen for all subsequent hydrolysis.

Hydrolysis conditions were further optimized with the prerequisite that complete dissolution of biological matrices (tissue) would be necessary for the method to be broadly applicable in biodistribution analyses. Incubation in 6 M H_2SO_4 at 105 °C for 24 h was therefore tested in both distilled water and rat liver homogenates before LC–QTOF analysis. The resulting ion spectra for all tested PEG compounds are shown in Fig. 2. The same PEG ions could be detected in all samples, with only minor changes in relative ion distribution – showing that the hydrolysis step successfully cleaved the different PEG conjugates. A

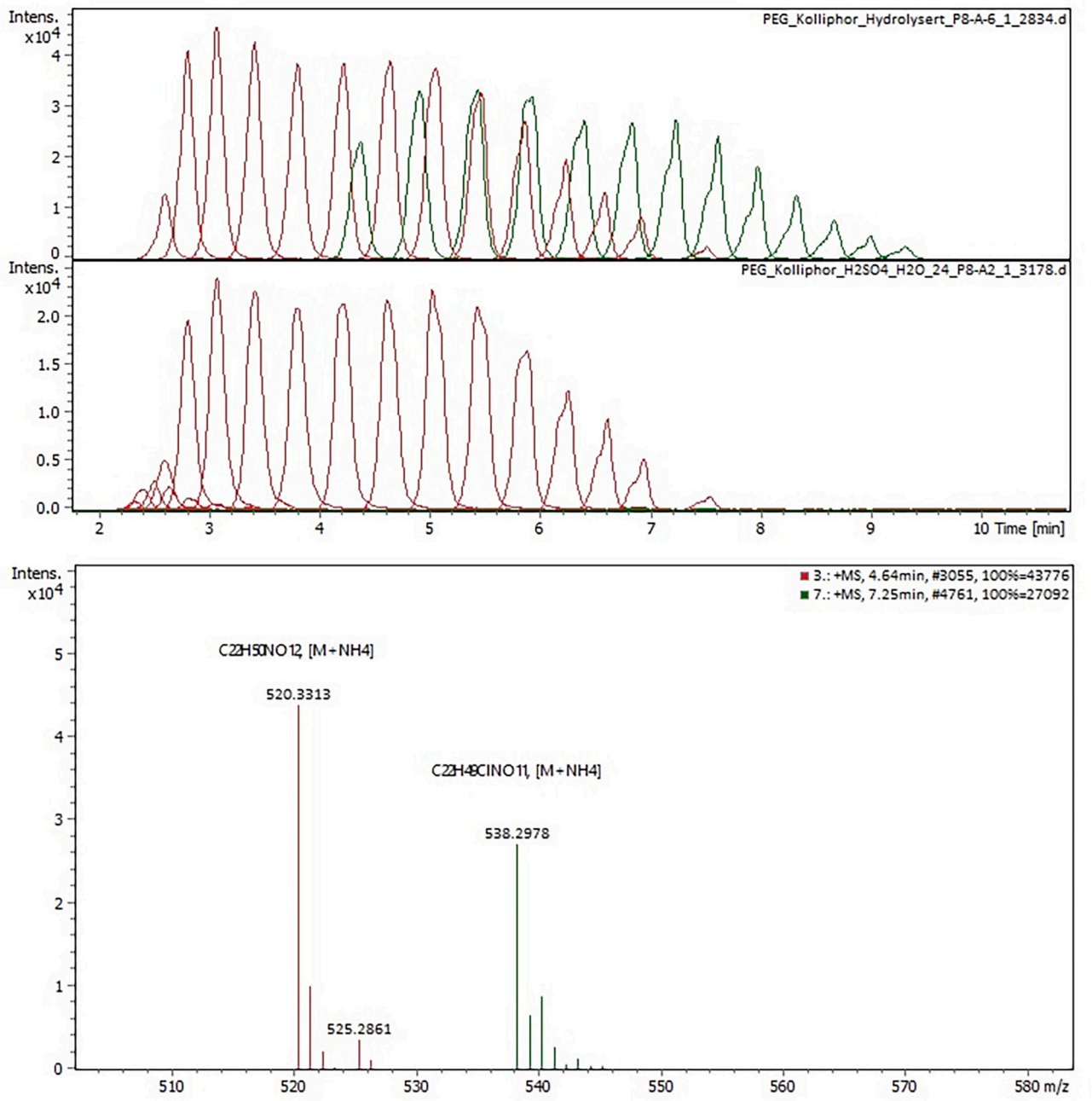

Fig. 1. LC–QTOF chromatograms showing Kolliphor HS15 hydrolyzed by (A) HCl and (B) H_2SO_4, with PEG-specific ions (red) and chlorinated PEG ions (green). (C) The mass spectrum of a representative PEG ion with and without chlorination. (For interpretation of the references to colour in this figure legend, the reader is referred to the web version of this article.)

comparison between 24 h and 48 h hydrolysis was also performed. Extending the incubation time to 48 h did not noticeably change mass spectral characteristics or ion intensities of the PEGylated compounds (Fig. S3), hence 24 h was found to be sufficient for complete tissue dissolution and PEG extraction. Nevertheless, hydrolysis times should be kept constant for comparative purposes, since some hydrolysis (scission) of the PEG chains will occur, and the optimal precursor ions are found to be in the mass ranges lower than that of the intact PEG (see below).

3.2. LC–MS/MS enables sensitive quantification of PEG hydrolysis products

Further LC–MS/MS method development was conducted to increase analyte specificity and sensitivity. Selected ions, corresponding to the ammonium adduct of linear PEG chains in the range of PEG9 to PEG25 (m/z 432 to 1136) were chosen as parent ions for quantitative analysis. The choice of the ammonium adduct as precursor was based on its superior abundance, as is commonly observed for PEG species. It is noteworthy that the best precursor ions after hydrolysis are below the mean PEG molecular weight of the parent PEG, indicating some PEG hydrolysis. A similar random chain scission effect is observed by Payne et al. (22) upon prolonged oxidative degradation of PEG, yielding a second PEG chain population with molecular weights in the 500–1200 Da range, from a starting PEG material with molecular weight average at approximately 2000 Da. Specific fragment ions were found by collision-induced dissociation, hence allowing for MRM analysis. Since all PEG

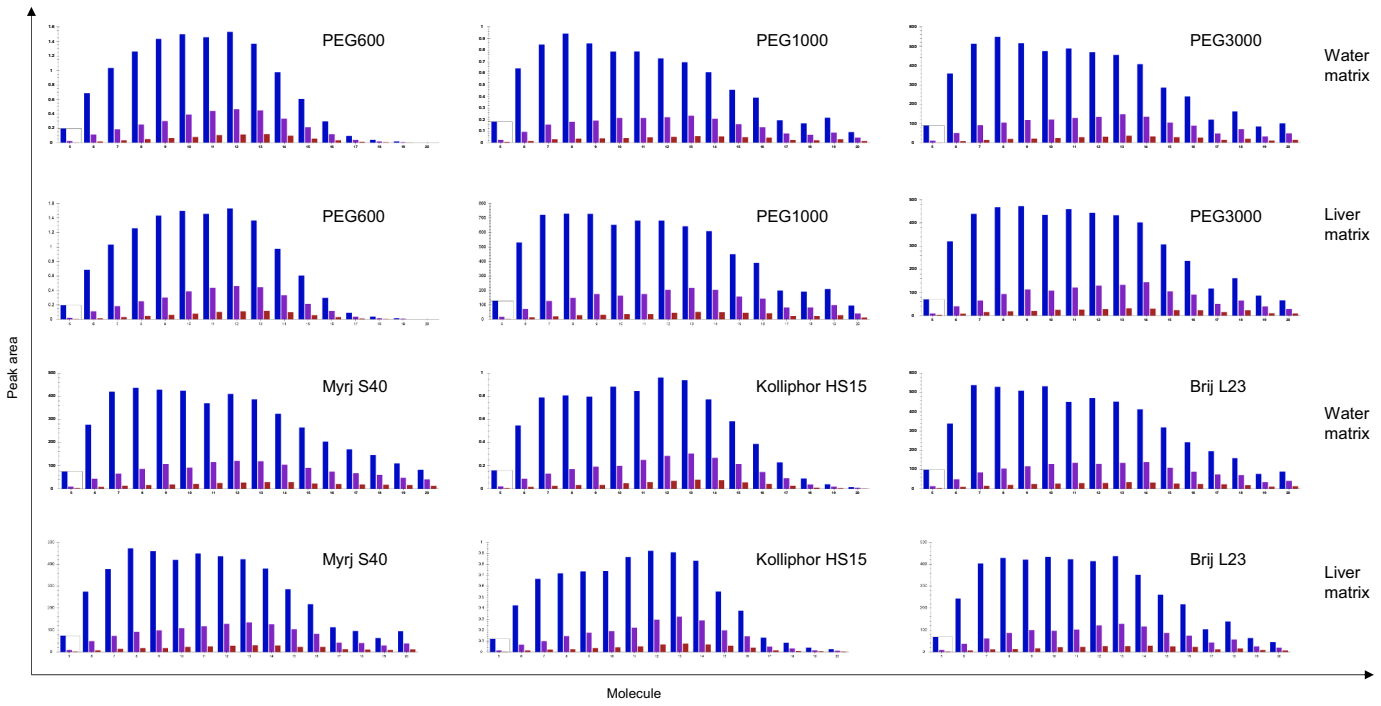

Fig. 2. Area comparison of different PEG chains from LC–QTOF analysis of PEGylated compounds spiked in water or liver homogenate matrices. All samples were hydrolyzed by H_2SO_4, 24 h incubation at 105 °C. The y-axes show peak area, the x-axes show PEG chain length distribution (as number of PEG units, PEG5-PEG20) and the different colored bars indicate the isotope pattern (blue bar: [M + NH4], purple bar: [M + NH4 + 1] and red bar: [M + NH4 + 2]). (For interpretation of the references to colour in this figure legend, the reader is referred to the web version of this article.)

molecules are essentially similar except for the different number of repeating oxyethylene units, the resulting fragments were similar for all parent ions. The *m/z* 89 ion was shown to be the most abundant fragment ion for all PEG parent ions, and therefore chosen as a common fragment for MRM analysis, and collision energy voltages for each transition were optimized.

3.3. PEG is a suitable, generic marker for a wide range of advanced therapeutics

Having established that the analytical approach was suitable for neat PEG chains and PEG conjugates, it was aimed to show its applicability to relevant therapeutics. This included analysis of Doxil®, Cimzia®, LNPs, LipImage (synthesized with the Myrj S40 PEG conjugate) and PEBCA-CBZ (synthesized with Kolliphor HS15 and Brij L23 PEG conjugates). LC–MS/MS chromatograms of these therapeutics after hydrolysis, referenced against a PEG1000 standard, are shown in Fig. 3. As seen, the main ions are common across all spectra, with only minor shifts in the relative ion distribution. This demonstrates the applicability of the proposed approach towards a wide range of PEGylated entities, independently of the molecule conjugated to the PEG polymer. It should be noted that all the above therapeutics, except Cimzia®, are nanoparticles. In the lipid-based systems, the PEG moiety is conjugated to a small molecule, whereas in the case of PEBCA, the conjugate partner is a large polymer. In the latter case, the total analyte molecular weight effectively prohibits molecular mass spectrometry analyses with relevant sensitivity, further demonstrating the value of the hydrolysis approach. Meanwhile, the results obtained for Cimzia® demonstrate that the current approach can be applied to PEGylated protein therapeutics, which is a rapidly expanding and highly promising class of medicines. Furthermore, Kolliphor HS15, used in the PEBCA formulation described here, is also broadly used in the clinic as a solubilizer for other poorly water soluble APIs, and is listed in US and European pharmacopeias as well as in the Inactive Ingredient Database (IID) (32). Finally, it should be noted that since formulation of the PEBCA-CBZ nanoparticles involve two different PEGylated compounds, it is not trivial to deconvolute their relative contributions to the total PEG signal, necessitating the use of the same particle material, rather than either of the pure PEGylated compounds alone, to build the quantification standard curves.

3.4. PEG can be robustly extracted from biological matrices

To fully characterize the fate and behavior of PEGylated entities after in vivo administration, a suitable extraction method is needed. This method should be simple, reproducible and broadly applicable to different tissue types. We hypothesized that hydrolysis of the tissue samples could fulfil these objectives. Tissue samples from a biodistribution study in rats (24) were therefore used as test samples in this proof-of-concept study. We included liver, spleen, kidney, heart and lung tissues, and blood plasma extracted from animals euthanized at different time points after intravenous injection of either LipImage or cabazitaxel-loaded PEBCA nanoparticles. As the tissues already were homogenized to extract and quantify the amount of IR780-oleyl or CBZ as described in (24), no sample preparation was needed before the hydrolysis step. Tissues from control animals injected with saline only were used to prepare PEG standard curves by adding known concentrations of LipImage or cabazitaxel-loaded PEBCA nanoparticles, the same formulations as used in the biodistribution study.

Sample hydrolysis resulted in visually different outcomes for the different tissue types, with varying degrees of sedimentation and transparency. Liver samples turned almost black, with visible sediments in all samples. Tissues from kidney, lung and heart turned brown with minor levels of sedimentation, while spleen samples turned light brown without any signs of sediments (Fig. S4). All samples were therefore filtered before pH adjustment and LC–MS/MS analysis. LC–MS/MS analysis showed that the different tissue matrices induced different levels of matrix effects, including background signals and ion suppression. The background signal of PEG varied between tissue, leading to varying limit of quantification (LOQ) levels (Table 2). This is expected to be a result of PEG accumulation in specific tissues due to PEG

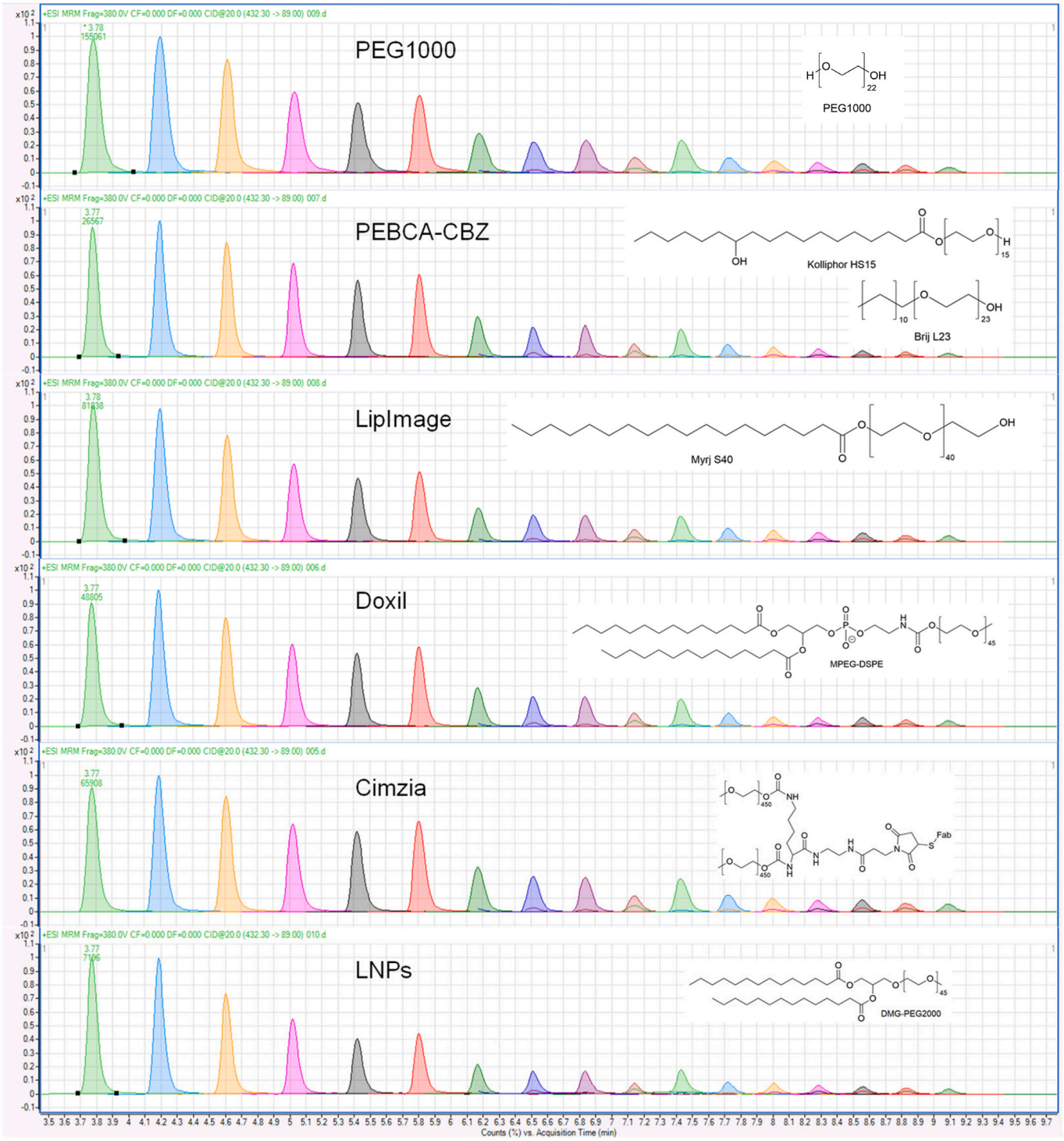

Fig. 3. LC–MS/MS chromatograms of the investigated PEGylated compounds after H_2SO_4 hydrolysis. Horizontal axis shows retention time (minutes) and vertical axes show signal intensity (counts) in the MS detection, normalized as % of the peak with highest intensity. Shading colors at given retention times represent identical PEG ions found across the sample set, to aid visualization.

contamination during animal rearing. In this study, the PEG background signals were shown to vary between the LipImage and PEBCA biodistribution studies. These experiments were performed at different animal facilities, emphasizing the impact of animal household on PEG contamination.

These differences in matrix effects emphasize the importance of preparing standard curves in the relevant matrix, e.g. liver tissue when quantitating PEG in liver samples. Matrix effects were also shown to vary between different PEG ions, leading to varying signal to noise ratios. A selection of the four transitions with the highest signal to noise ratio was therefore chosen and averaged for quantification. For LipImage, the *m/z* 740, 784, 828 and 872 ions (corresponding to PEG 16–19) were selected, while the m/z 652, 696, 740 and 784 ions (corresponding to PEG 14–17) were used for PEBCA nanoparticles.

Overall, there are at least five conceivable sources of variability in the current method; i) incomplete hydrolysis of the PEG moiety from the

Table 2
LOQ levels in different organs. The concentration levels correspond to the lowest amount of LipImage or PEBCA-CBZ that could be quantified in tissue from untreated rats spiked with the formulation. The LOQ levels in spiked blank samples (H2O) are included for reference.

	LipImage	PEBCA-CBZ
Liver	1 μg/mL	0.5 μg/mL
Spleen	1 μg/mL	1 μg/mL
Kidneys	1 μg/mL	1 μg/mL
Lungs	5 μg/mL	1 μg/mL
Heart	10 μg/mL	1 μg/mL
Plasma	1 μg/mL	300 μg/mL
Blank (H2O)	0.1 μg/mL	0.1 μg/mL

conjugate, ii) degradation of the PEG moiety during hydrolysis, iii) incomplete tissue extraction, iv) loss during sample processing and v) analytical interference during ionization of the analytes. We would argue that the strategy chosen in the current work will minimize the variability from all these factors. This strategy builds the standard curves for quantification with the (nanoformulated) analyte in each of the relevant tissue homogenates, and includes the complete H_2SO_4 hydrolysis process with the same hydrolysis exposure times. Furthermore, it performs quantification relative to the complete nanoformulation as such, rather than the single constituent compounds. Importantly, all the standard curves used for quantification in the tissue samples (see below) showed excellent linearity ($R^2 > 0.995$, all ions, quadratic curve fit). These standard curves encompass the spiking of tissue homogenates with different concentrations of the nanoparticles before hydrolysis, thus covering both the chemical conversion and the the tissue extraction. Thus, extraction efficiency can be considered essentially constant across all relevant concentrations.

3.5. *PEG biodistribution in tissue reveals different drug release kinetics from nanomedicines in vivo*

In the beforementioned biodistribution study, the small molecule payloads were quantified as proxies for biodistribution of the nanoformulations LipImage and PEBCA-CBZ (24). In both cases, the payload is assumed to be only entrapped in the particle matrix during encapsulation, and not covalently attached to it. Several notable differences were observed in the biodistribution of the two formulations, with the most pronounced difference being a much (>50-fold) higher measured concentration ratio between CBZ and PEBCA in all organs vs. blood, as compared to that of IR780-oleyl and LipImage. This and other effects could conceivably be related to differences in nanoparticle payload release rates and nanoparticle stability in circulation and in organs. These observations are inherently difficult to explain without a way to directly measure both the nanoparticle and its payload independently. The PEG methodology described in the current work was therefore used to quantitate the amount of PEG in the existing samples from the previous study, as a proxy for the amount of nanoparticle carrier. The results are summarized in Fig. 4 and will be elaborated in the following.

Some striking differences between the two nanoparticle systems are seen in terms of PEG/payload ratio. For liver, although the time profile of the PEG signal is similar for both particles, the payload time profiles are very different. This is explicitly visualized as PEG/payload signal ratios in Fig. 5. Whereas the ratio of PEG to payload actually increases in the case of PEBCA-CBZ up to 9 h, the same ratio is strongly and uniformly decreasing already from the first sampling point in the case of LipImage. The rapid elimination of PEG relative to IR780-oleyl from the administered LipImage suggests the rapid and thorough dissociation of the particles. Alternatively, it represents shedding of the PEG-stearate. Considering the relatively high proportion of PEG-stearate (almost 50% of total lipids) in the formulation, this would likely lead to a major reorganization or dissolution of the particles. Whether the remaining lipids are eliminated at the same rate as PEG-stearate cannot be determined with the present method, and this is inherently difficult to quantify as the majority of the remaining lipids are endogenously present in cells. The opposite time development, seen with PEBCA-CBZ, however, could indicate release of CBZ from relatively intact and retained nanoparticles. Nevertheless, the first two sampling points (1 h, 1 day represent an interesting situation where the detected concentrations of PEG relative to CBZ is *lower* than in the intact nanoformulation injected. Two factors could conceivably contribute to this observation. Firstly, the first sampling point is at 1 h, i.e. potentially allowing for some release and redistribution to already occur. Secondly, provided a certain burst release of CBZ takes place in the blood, released CBZ – which is very hydrophobic – could be taken up in the liver, adding to the dose encapsulated in the PEBCA nanoparticles. Co-administration of the nanoformulation with free CBZ or PEGylated compounds could conceivably be a way to investigate this hypothesis in future studies.

In spleen, the PEG/payload time profiles are even more different; no PEG signal could be detected in the PEBCA-CBZ case, but the concentration of CBZ showed a roughly exponential decline. In the LipImage case, however, the ratio is inverted over time, with the IR780-oleyl payload exhibiting a much longer relative persistence in the tissue. It is interesting to note that the decrease in concentration of both PEG and payload from LipImage is slower in spleen than in liver. This could indicate a relatively higher particle stability in the spleen tissue environment. In kidneys, there is a high accumulation of CBZ relative to PEG, whereas for LipImage, the early accumulationof PEG and IR780-oleyl is relatively similar, but prolonged for the latter. In heart tissue, CBZ/PEG sems to follow a similar trend, whereas IR780-oleyl does not noticeably accumulate. In lungs, PEG from LipImage accumulates in proportional manner to IR780-oleyl. In addition, it is interesting to note the relative distribution of the different components at the earliest time point, for the two nanoparticle systems, measured as concentration in the respective tissues: For PEBCA-CBZ, the highest (and almost exclusive) concentration of PEG is in the liver, whereas the CBZ payload is most concentrated in the lungs. For LipImage, on the other hand, PEG is found at highest concentration in spleen and heart, and the IR780-oleyl payload is most concentrated in the liver.

Finally, in plasma, both payloads are cleared rapidly, and are only seen at the earliest time point (Fig. S5). PEG stemming from LipImage was not observed in the plasma. We did detect significant amounts of PEG from the PEBCA-CBZ formulation; this data was, however, not possible to use for quantification as it was observed a high background level of PEG in the blank samples (Table 2). This PEG was found to originate from the blood sampling tubes used in the PEBCA-CBZ experiment (but not in the LipImage experiment), and this very clearly illustrates one key consideration that must be made using the current method. PEGylated compounds are very widely used throughout manufacturing of a lot of items, and this must be tested for (and avoided) in all sample handling operations to be applied.

As is frequently the case in biodistribution studies, total recovered dose in the selection of organs analyzed does not add up to the initial administered dose (see Fig. S6). Several factors could contribute to this, beyond the overall limited selection of organs and the remaining body tissue not investigated here, such as e.g. the blood vessels. Urine and feces were not collected in the current study and API metabolites and degradation products were not quantified here. Importantly, quantification in blood is likely to be incomplete. In pharmacokinetic and biodistribution studies, quantification is frequently performed in plasma or serum, i.e. after removal of circulating blood cells. Recent work could indicate that this leads to loss of significant amounts of injected nanoparticles, both by red blood cells (33) and circulating immune cells (34). We would therefore propose that future studies could include quantification in both whole blood and plasma/serum.

We present here a methodology that should enable more detailed insight into pharmacokinetic and biodistribution analyses of most nanomedicines and numerous other PEGylated therapeutics. Importantly, this can be obtained without any increase in the number of

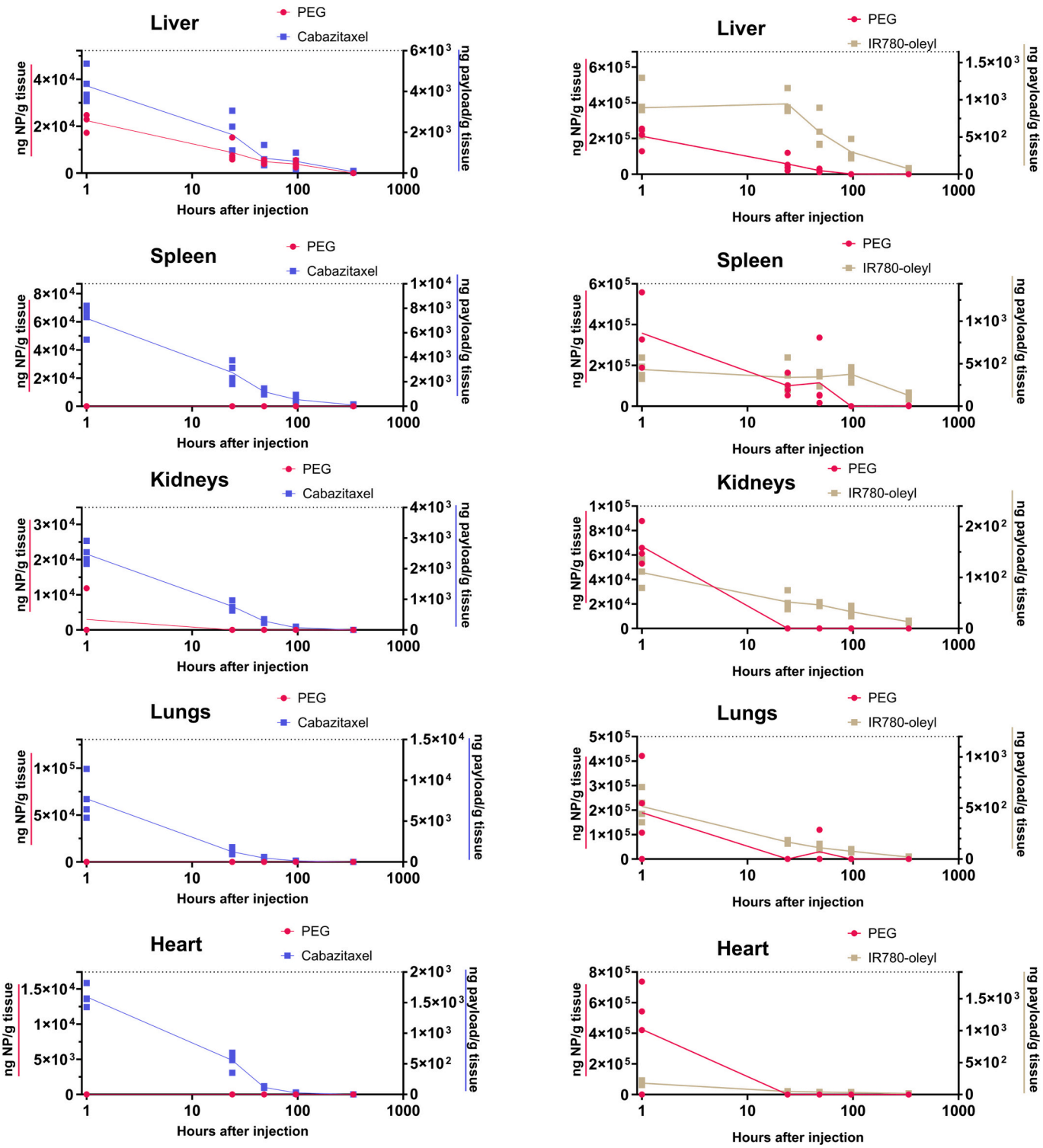

Fig. 4. Biodistribution of PEBCA-CBZ (left panels) and LipImage (right panels) in rats. Nanoparticles are quantified as PEG equivalents. For all panels, the horizontal (time) axis has been plotted logarithmically, to better visualize the earliest sampling points where most of the changes are observed. The right and left vertical axes scales are locked in a fixed ratio (per particle type) that reflects the relative concentrations of nanoparticles (as PEG, left) vs. nanoparticle payload (right) in the dispersion that was administered, i.e. the ratio before any physiological conversion of the nanoparticle formulation had taken place. Thus, a perfectly intact and unchanged nanoparticle would give completely superimposed data points for the PEG and the payloads. Note that absolute values vary between the subgraph vertical axes to optimize readability. Payload data was previously published by the authors in (24) and is reused under CC license.

animals used, simply by performing more analyses on existing samples. This inherently minimizes both biological and analytical variability. The method described is shown to be very generic and broadly applicable across tissue types and therapeutics with different PEG conjugates. Moreover, it could conceivably be used for safety studies on exposure to both therapeutic and non-therapeutic PEGylated compounds, such as cosmetics. Furthermore, the concept of complete chemical dissolution of the sample matrix by hydrolysis combined with the high analytical

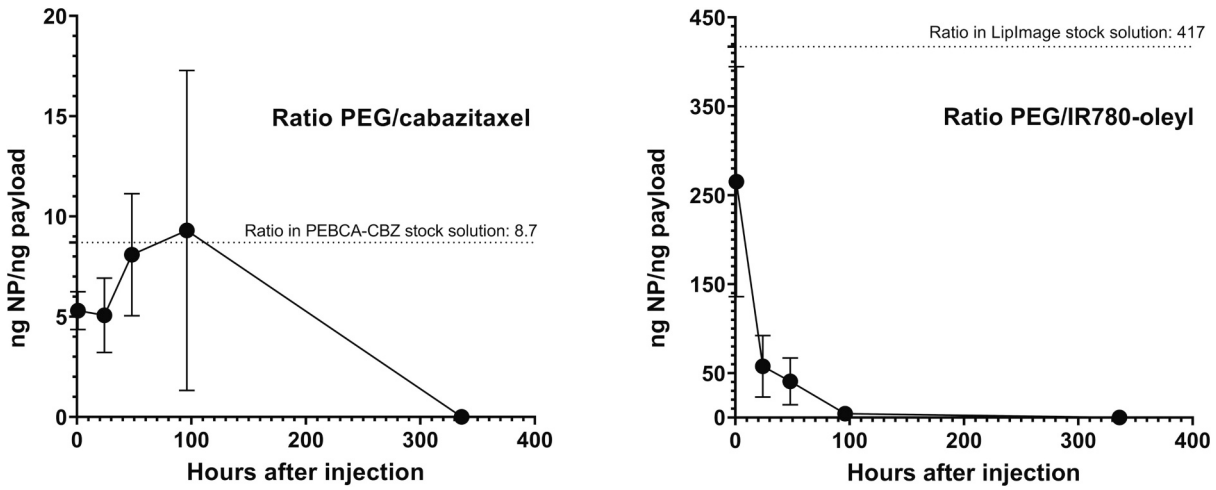

Fig. 5. Nanoparticle/payload ratios in liver tissue for PEBCA-CBZ (left graph) and LipImage (right graph). Dotted lines indicate ratios in original formulations prior to injection. Nanoparticles are quantified as PEG equivalents.

performance of LC–MS/MS should provide near-optimal sensitivity. We do, however, observe residual matrix effects even after hydrolysis. This points to the need for further method optimization and the need to perform quantification against matrix-matched standard curves. The current method is investigational in nature, and a full, formal method validation is considered beyond the scope of the current work. Nevertheless, future work should aim to both perform such validation, and concomitantly do a detailed investigation of sources of variability in the sample preparation and analysis.

It should be pointed out that the same sample preparation and analytical principles as described here could be applied to PEG alternatives. The ongoing assessment of possible adverse immune reactions to PEG has spurred interest in other chemical moieties that could serve the same function, such as polyglycerols or zwitterionic polymers (recently reviewed in e.g. (13) and (35)). The requirement would be sufficient stability under the chosen hydrolysis conditions, and the creation of non-endogenous, detectable molecular fragments. We also observe that the methodology proposed here could be applied on the cellular level, to assess nanomedicine uptake and conversion in cell populations such as circulatory immune cells, e.g. by performing fluorescence-activated cell sorting (FACS) followed by quantification of the API and PEG in the isolated cell populations.

Although stable PEGylation is generally desirable in order to improve in vivo nanoparticle performance, it is important to note that some nanomedicines are designed to shed their exposed PEG moieties. This is the case for e.g. the LNP-based formulation used in Onpattro®, where shedding of PEG induces the recruitment of the endogenous apolipoprotein ApoE from the blood stream, in turn facilitating uptake of the LNPs into the target hepatic cells by low-density-lipoprotein receptors and other ApoE-dependent uptake mechanisms (36). Building a methodology that could also quantify other (non-API, non-PEG) components of the nanoformulation under study could help quantify such PEG loss. Candidates for such compounds should be non-endogenous, e.g. the (semi-)synthetic ionizable lipids used in LNPs, and, ideally, metabolically inert.

4. Conclusion

In summary, we developed a robust and versatile approach for quantitative analysis of PEGylated therapeutics in biological matrices. A wide variety of PEG compounds was successfully hydrolyzed into specific PEG-fragments, detectable by LC–MS/MS. Method applicability in biodistribution studies was further demonstrated by quantitating PEG in plasma and tissue homogenates from a previous rat biodistribution study. We demonstrate that its use in tandem with nanoparticle payload quantification allows for probing in vivo nanoparticle stability and drug release. Finally, we propose that quantification of PEG, where applicable, could be performed in preexisting samples and future preclinical evaluation of candidate therapeutics in order to support their safety assessment and accelerated clinical translation.

CRediT authorship contribution statement

Astrid Hyldbakk: Writing – original draft, Visualization, Methodology, Investigation, Formal analysis. **Terkel Hansen:** Writing – review & editing, Visualization, Methodology. **Sjoerd Hak:** Writing – review & editing, Conceptualization. **Sven Even F. Borgos:** Writing – original draft, Project administration, Methodology, Funding acquisition, Conceptualization.

Data availability

Data will be made available on request.

Acknowledgements

This work was received funding from the European Union's Horizon 2020 Research and Innovation Programme under grant agreement no 761104 (REFINE) and 825828 (EXPERT). The authors thank the REFINE consortium for providing PEBCA and LipImage formulations, and for the biodistribution samples. Additionally, Jérémie Parot synthesized the LNPs, Kai Vernstad contributed to the LC–MS/MS methodology, Karina Sletvik participated in tissue sample hydrolysis and Peter Molesworth contributed to the design of the hydrolysis step.

Declaration of competing interest

The authors declare no competing interests.

Appendix A. Supplementary data

Supplementary data to this article can be found online at https://doi.org/10.1016/j.jconrel.2024.01.016.

References

[1] Y. Chezy Barenholz, Doxil® — the first FDA-approved nano-drug: lessons learned, J. Control. Release 160 (2) (2012 Jun 10) 117–134.

[2] WHO Coronavirus (COVID-19) Dashboard [Internet], Available from: https://covid19.who.int, 2022 Dec 8.
[3] O.J. Watson, G. Barnsley, J. Toor, A.B. Hogan, P. Winskill, A.C. Ghani, Global impact of the first year of COVID-19 vaccination: a mathematical modelling study, Lancet Infect. Dis. 22 (9) (2022 Sep 1) 1293–1302.
[4] J. Minnema, S.E.F. Borgos, N. Liptrott, R. Vandebriel, C. Delmaar, Physiologically based pharmacokinetic modeling of intravenously administered nanoformulated substances, Drug Deliv. Transl. Res. 12 (9) (2022 Sep 1) 2132–2144.
[5] R.K.R. Rajoli, D.J. Back, S. Rannard, C.L. Freel Meyers, C. Flexner, A. Owen, et al., Physiologically based pharmacokinetic modelling to inform development of intramuscular long-acting Nanoformulations for HIV, Clin. Pharmacokinet. 54 (6) (2015 Jun 1) 639–650.
[6] S. Skoczen, S.E. McNeil, S.T. Stern, Stable isotope method to measure drug release from nanomedicines, J. Control. Release 220 (2015) 169–174.
[7] S.L. Skoczen, K.S. Snapp, R.M. Crist, D. Kozak, X. Jiang, H. Liu, et al., Distinguishing pharmacokinetics of marketed nanomedicine formulations using a stable isotope tracer assay, ACS Pharmacol. Transl. Sci. 3 (3) (2020 Jun 12) 547–558.
[8] A.A. D'Souza, R. Shegokar, Polyethylene glycol (PEG): a versatile polymer for pharmaceutical applications, Expert Opin. Drug Deliv. 13 (9) (2016 Sep) 1257–1275.
[9] P.L. Turecek, M.J. Bossard, F. Schoetens, I.A. Ivens, PEGylation of biopharmaceuticals: a review of chemistry and nonclinical safety information of approved drugs, J. Pharm. Sci. 105 (2) (2016 Feb) 460–475.
[10] Z. Zhang, Y. Zhang, S. Song, L. Yin, D. Sun, J. Gu, Recent advances in the bioanalytical methods of polyethylene glycols and PEGylated pharmaceuticals, J. Sep. Sci. 43 (9–10) (2020 May 1) 1978–1997.
[11] A. Kolate, D. Baradia, S. Patil, I. Vhora, G. Kore, A. Misra, PEG - a versatile conjugating ligand for drugs and drug delivery systems, J. Control. Release 192 (2014 Oct 28) 67–81.
[12] FDA Approved PEGylated Drugs Up To 2022 | Biopharma PEG [Internet], Available from: https://www.biochempeg.com/article/58.html, 2022 Dec 16.
[13] D. Shi, D. Beasock, A. Fessler, J. Szebeni, J.Y. Ljubimova, K.A. Afonin, et al., To PEGylate or not to PEGylate: immunological properties of nanomedicine's most popular component, polyethylene glycol and its alternatives, Adv. Drug Deliv. Rev. 180 (2022 Jan 1) 114079.
[14] Z. Hussain, S. Khan, M. Imran, M. Sohail, S.W.A. Shah, M. de Matas, PEGylation: a promising strategy to overcome challenges to cancer-targeted nanomedicines: a review of challenges to clinical transition and promising resolution, Drug Deliv. Transl. Res. 9 (3) (2019 Jun) 721–734.
[15] G.T. Kozma, T. Mészáros, P. Berényi, R. Facskó, Z. Patkó, C.Z. Oláh, et al., Role of anti-polyethylene glycol (PEG) antibodies in the allergic reactions to PEG-containing Covid-19 vaccines: evidence for immunogenicity of PEG, Vaccine. 41 (31) (2023 Jul 12) 4561–4570.
[16] M. Ibrahim, E. Ramadan, N.E. Elsadek, S.E. Emam, T. Shimizu, H. Ando, et al., Polyethylene glycol (PEG): the nature, immunogenicity, and role in the hypersensitivity of PEGylated products, J. Control. Release 351 (2022 Nov 1) 215–230.
[17] H. Kang, S. Rho, W.R. Stiles, S. Hu, Y. Baek, D.W. Hwang, et al., Size-dependent EPR effect of polymeric nanoparticles on tumor targeting, Adv. Healthc. Mater. 9 (1) (2020) 1901223.
[18] X. Hou, T. Zaks, R. Langer, Y. Dong, Lipid nanoparticles for mRNA delivery, Nat. Rev. Mater. 6 (12) (2021 Dec) 1078–1094.
[19] A.P. Dias, Santos S. da Silva, J.V. da Silva, R. Parise-Filho, E. Igne Ferreira, O. E. Seoud, et al., Dendrimers in the context of nanomedicine, Int. J. Pharm. 573 (2020 Jan 5) 118814.
[20] I. Alberg, S. Kramer, M. Schinnerer, Q. Hu, C. Seidl, C. Leps, et al., Polymeric nanoparticles with neglectable protein Corona, Small. 16 (18) (2020) 1907574.
[21] X. Shan, X. Gong, J. Li, J. Wen, Y. Li, Z. Zhang, Current approaches of nanomedicines in the market and various stage of clinical translation, Acta Pharm. Sin. B 12 (7) (2022 Jul 1) 3028–3048.
[22] M.E. Payne, O.O. Kareem, K. Williams-Pavlantos, C. Wesdemiotis, S.M. Grayson, Mass spectrometry investigation into the oxidative degradation of poly(ethylene glycol), Polym. Degrad. Stab. 183 (2021 Jan 1) 109388.
[23] G. Berrecoso, J. Crecente-Campo, M.J. Alonso, Quantification of the actual composition of polymeric nanocapsules: a quality control analysis, Drug Deliv. Transl. Res. 12 (11) (2022 Nov 1) 2865–2874.
[24] A.K.O. Åslund, R.J. Vandebriel, F. Caputo, W.H. de Jong, C. Delmaar, A. Hyldbakk, et al., A comparative biodistribution study of polymeric and lipid-based nanoparticles, Drug Deliv. Transl. Res. 15 (2022 Apr) 1–18.
[25] S. Snipstad, Ý. Mørch, E. Sulheim, A. Åslund, A. Pedersen, C.L. de Davies, et al., Sonopermeation enhances uptake and therapeutic effect of free and encapsulated Cabazitaxel, Ultrasound Med. Biol. 47 (5) (2021 May 1) 1319–1333.
[26] M. Fusser, A. Øverbye, A.D. Pandya, Ý. Mørch, S.E. Borgos, W. Kildal, et al., Cabazitaxel-loaded poly(2-ethylbutyl cyanoacrylate) nanoparticles improve treatment efficacy in a patient derived breast cancer xenograft, J. Control. Release 293 (2019 Jan 10) 183–192.
[27] A. Jacquart, M. Keramidas, J. Vollaire, R. Boisgard, G. Pottier, E. Rustique, et al., LipImageTM 815: novel dye-loaded lipid nanoparticles for long-term and sensitive in vivo near-infrared fluorescence imaging, JBO. 18 (10) (2013 Jul) 101311.
[28] R. Mildner, S. Hak, J. Parot, A. Hyldbakk, S.E. Borgos, D. Some, et al., Improved multidetector asymmetrical-flow field-flow fractionation method for particle sizing and concentration measurements of lipid-based nanocarriers for RNA delivery, Eur. J. Pharm. Biopharm. 163 (2021 Jun 1) 252–265.
[29] J. Gong, X. Gu, W.E. Achanzar, K.D. Chadwick, J. Gan, B.J. Brock, et al., Quantitative analysis of polyethylene glycol (PEG) and PEGylated proteins in animal tissues by LC–MS/MS coupled with in-source CID, Anal. Chem. 86 (15) (2014 Aug 5) 7642–7649.
[30] H. Li, M.J. Rose, J.R. Holder, M. Wright, L.P. Miranda, C.A. James, Direct quantitative analysis of a 20 kDa PEGylated human calcitonin gene peptide antagonist in Cynomolgus Monkey serum using in-source CID and UPLC–MS/MS, J. Am. Soc. Mass Spectrom. 22 (9) (2011 Sep 1) 1660–1667.
[31] L. Huang, P.C. Gough, M.R. Defelippis, Characterization of poly(ethylene glycol) and PEGylated products by LC/MS with postcolumn addition of amines, Anal. Chem. 81 (2) (2009 Jan 15) 567–577.
[32] Shaukat Ali, Kolliphor® HS 15 - An Enabler for Parenteral and Oral Formulations [Internet] [cited 2023 Feb 7]. Available from: http://www.americanpharmaceuticalreview.com/Featured-Articles/358749-Kolliphor-HS-15-An-Enabler-for-Parenteral-and-Oral-Formulations/, 2019.
[33] J.S. Brenner, S. Mitragotri, V.R. Muzykantov, Red blood cell hitchhiking: a novel approach for vascular delivery of Nanocarriers, Annu. Rev. Biomed. Eng. 23 (1) (2021) 225–248.
[34] A.M. Sofias, Y.C. Toner, A.E. Meerwaldt, M.M.T. van Leent, G. Soultanidis, M. Elschot, et al., Tumor targeting by αvβ3-integrin-specific lipid nanoparticles occurs via phagocyte hitchhiking, ACS Nano 14 (7) (2020 Jul 28) 7832–7846.
[35] T.T. Hoang Thi, E.H. Pilkington, D.H. Nguyen, J.S. Lee, K.D. Park, N.P. Truong, The importance of poly(ethylene glycol) alternatives for overcoming PEG immunogenicity in drug delivery and bioconjugation, Polymers. 12 (2) (2020 Feb) 298.
[36] A. Akinc, M.A. Maier, M. Manoharan, K. Fitzgerald, M. Jayaraman, S. Barros, et al., The Onpattro story and the clinical translation of nanomedicines containing nucleic acid-based drugs, Nat. Nanotechnol. 14 (12) (2019 Dec) 1084–1087.